Landau–de Gennes theory of the chevron structure in a smectic liquid crystal

N. Vaupotič,[1] S. Kralj,[1] M. Čopič,[2] and T. J. Sluckin[3]
[1]*Department of Physics, Faculty of Education, University of Maribor, Maribor, Slovenia*
[2]*Department of Physics and Jožef Stefan Institute, University of Ljubljana, Ljubljana, Slovenia*
[3]*Department of Mathematics, University of Southampton, Southampton SO17 1BJ, United Kingdom*
(Received 14 May 1996)

The covariant form of the Landau–de Gennes free energy is used to study the chevron structure formed by cooling from the Sm-*A* to the nonchiral Sm-*C* phase in a surface-stabilized cell with planar boundary conditions. We show that the chevron is the thermodynamic equilibrium structure. The chevron structure is studied depending on the liquid-crystal elastic properties, temperature, and the surface orientational anchoring strength. We show that the bistability of the chevron structure results from the continuity of the molecular director over the chevron tip of finite width, and is strongly dependent on the surface orientational anchoring. We estimate analytically the threshold temperature for the chevron formation and show that above this temperature the bookshelf geometry is stable. We show that the energy of the chevron interface follows a power-law dependence on reduced temperature with the exponent of $\frac{3}{2}$. [S1063-651X(96)09110-6]

PACS number(s): 61.30.Jf, 64.70.Md

I. INTRODUCTION

The chevron structure can be observed in thin cells of Sm-*C* liquid crystal, either chiral or nonchiral, when a cell filled with Sm-*A* liquid crystal is cooled into the Sm-*C* phase [1,2]. It is a widespread feature in ferroelectric Sm-$C^{\star}$ cells with optical device applications. The chevron is believed to be a consequence of the mismatch between the periodicity imposed by the surface and the periodicity imposed by the bulk liquid crystal. In many experimental contexts [3] once the layers are formed in the Sm-*A* phase, the surface positional anchoring is frozen in and the layers do not move along the glass plates. In this case the only way to simultaneously maintain the periodicity of the Sm-*A* liquid crystal along the boundary plates and reduce the layer thickness is to tilt the layers away from the normal to the bounding plates.

There has already been extensive work on the theory of the layer and director structure in varying alignment and applied field conditions in ferroelectric Sm-*C* liquid crystals. The local liquid-crystal structure is described in terms of the molecular cone angle (ϑ), the layer tilt angle (δ), and the angle describing the director rotation about the cone (φ) [Fig. 1(b)]. Clark and co-workers [1,4] have assumed that the chevron tip is sharp and have thus neglected the detailed structure of the layers at the chevron tip. In their model the molecular director is continuous over the cell. They have assumed that the layer tilt angle is constant (δ_0) and smaller than the molecular cone angle (ϑ_0). This leads to director pretilt; the director at the surface becomes inclined with respect to the cell plane at an angle $\pm\varphi_0$, where $\sin\varphi_0=\tan\delta_0/\tan\vartheta_0$. As soon as the director tilts away from the cell plane, there are two distinct stable director states with the same free energy. This bistability is very important and is used in optical applications, where the cell is switched between the stable states, i.e., between a dark and a bright state. The description has later been extended to include the effects of the electric field [5–7].

However, treating the chevron tip as sharp leaves open the question of the chevron tip structure. Nakagawa [8] proposed a model that takes into account dilatation and bending of the layers and the director rotation about the cone. In this approach the sharp tip is replaced by a localized folding, associated with a solitonlike solution. His solution is valid when the angles ϑ, δ, and φ are small. A simplified form of Nakagawa's expression for the free-energy density [9] was used by Sabater *et al.* to study the chevron structures in the case of large angles [10]. In all the above models the molecular cone angle was kept constant and the bulk value of the layer tilt angle was assumed to be smaller than the molecular cone angle. De Meyere and co-workers [11,12] have used a related strategy, in which spatial variations of the molecular cone angle were also taken into account. In their work the molecular cone angle and the layer tilt angle are coupled. The coupling parameter is defined by the way in which the transition from the Sm-*A* to the Sm-*C* phase occurred. Their

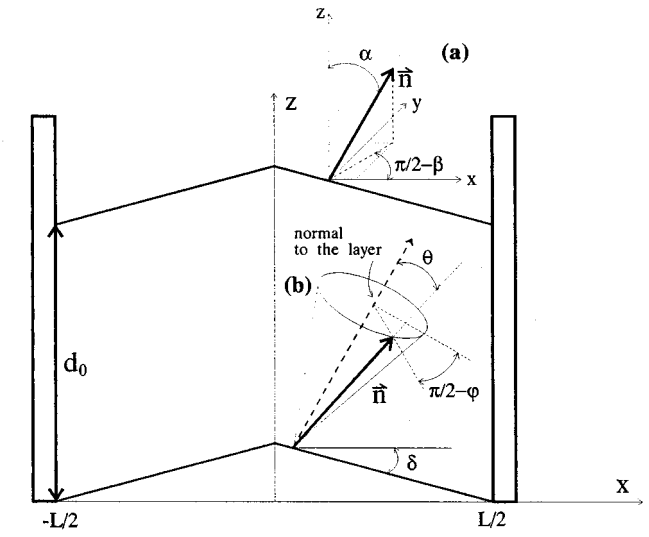

FIG. 1. (a) The coordinate system in which the numerical calculations were performed. (b) The coordinate system used to describe the chevron structure.

expression is based on the Dahl-Lagerwall description of the Sm-$C^\star$ elasticity [13,14].

Recently, Limat [15] proposed a simplified model of the chevron structure based on a generalization of the ''uniaxial'' (or ''nematic'') approximation of the orientational elasticity. Two parameters are introduced measuring the departure from the uniaxial approximation, and the molecular cone angle is taken to be constant. When the bulk value of layer tilt angle is small compared to the molecular cone angle and in the case of the uniform states, this model reduces to Nakagawa's soliton solution. The sharp chevron tip discontinuity characteristic of the model of Clark and co-workers is obtained in the uniaxial limit.

In this paper we use the Landau–de Gennes theory to show that the chevron is the equilibrium structure of the Sm-*C* phase in thin layers with planar boundary conditions. The model is conceptually quite simple, but still allows us to study all the essential features of the structure. We describe the Sm-*C* phase in terms of the director field $\mathbf{n}(\mathbf{r})$ and the complex smectic density wave $\psi(\mathbf{r})$, as proposed by de Gennes [16] and Lubensky [17]. In our view, with respect to other available models, our model has computational and conceptual advantages for describing the chevron structure. Conceptually we retain the simplicity of the model of Clark and co-workers. Computationally, we shall find that many of the simplifying assumptions employed in other models of this phenomenon are no longer required in our model.

The central assumption of the previous models is that the equilibrium layer tilt angle (δ_0) is smaller than the equilibrium molecular cone angle (ϑ_0). This has been a necessary condition to obtain a finite pretilt of the molecular director. Optical bistability, which is necessary for switching in surface-stabilized chevron liquid-crystal cells, requires a finite pretilt. By contrast, we show that $\delta_0 < \vartheta_0$ is not a necessary condition to obtain the pretilt of the director.

In our approach, all three relevant angles are treated as variational parameters. In other models ϑ is either kept constant or is coupled to δ by $\cos\vartheta = \nu\cos\delta$, $\nu = \text{const} < 1$. By comparison with the results of other models of the same phenomenon, we find that

(i) The model of Clark *et al.* works well deep in the Sm-*C* phase.

(ii) We obtain results for the spatial variation of the layer tilt angle similar to those of De Meyere and co-workers.

(iii) Limat has shown that in the limit of his model Nakagawa's soliton solution is valid only when $\delta_0 \ll \vartheta_0$. We show how Limat's two parameters that measure the departure from the uniaxial approximation can be expressed using the smectic elastic constants entering our model.

(iv) Leslie and co-workers [18,19] have proposed a rather general free-energy density expression for the Sm-*C* phase. This expression is written in terms of the **a**, **b**, **c** vectors, and contains all the invariants of the Sm-*C* phase. This approach is modeled on classical continuum mechanics, and is awkwardly generalized to discuss variations in the layer thickness and changes in molecular tilt with respect to the layer normal. It is rather comprehensive. The main advantage of our approach is that it explicitly focuses on layer displacement in a problem for which the boundary conditions are expressed in terms of zero layer displacement. We are also able to treat the temperature dependence of the structure, in particular the transition from the Sm-*A* phase.

We emphasize that we need only four elastic constants to describe the main features of the chevron structure. To describe the effects of the surface an additional term is needed. We present a simple but thorough study of the effect of the surface anchoring conditions on the chevron structure, especially on the pretilt of the molecular director. Our model also enables us to study the temperature dependence of the chevron structure. We show that the chevron structure is not formed immediately below the Sm-*A*–Sm-*C* transition temperature and we shall estimate analytically the threshold temperature for the chevron formation.

Spatial variations of the smectic order parameter can also readily be taken into account using our model, but we postpone this aspect to future work. In this paper we stay well inside the smectic phase where spatial variations of the smectic order parameter are expected to be negligible.

The plan of the paper is as follows. In Sec. II we introduce the model. In Sec. III we show the numerical results for the spatial variation of all the variational parameters and the free-energy density in the chevron. We calculate the excess free energy associated with the chevron interface. We also analytically estimate the threshold temperature for the chevron formation. Then we compare our results with other models. In Sec. IV we draw some brief conclusions.

II. MODEL

The Sm-*C* phase is described in terms of the director field $\mathbf{n}(\mathbf{r})$ and the complex smectic density wave $\psi(\mathbf{r}) = \eta(\mathbf{r})\exp[i\phi(\mathbf{r})]$. The latter is related to the first harmonic of the density deviation from the homogeneous distribution. The phase factor $\phi(\mathbf{r})$ determines the position of the layers, with $\boldsymbol{\nu} = \nabla\phi/|\nabla\phi|$ the layer normal direction. The scalar smectic order parameter $\eta(\mathbf{r})$ describes the degree of layer ordering. Throughout the following work it is kept constant and equal to its bulk value η_B. We thus assume that local smectic elastic distortions are not strong enough to cause significant variation in $\eta(\mathbf{r})$.

The free energy of a Sm-*C* cell can be written as a sum of the nematic, smectic, and surface contributions [16,17,20]:

$$F = \int [f_n(\mathbf{r}) + f_s(\mathbf{r})]d^3\mathbf{r} + \int f_a(\mathbf{r})d^2\mathbf{r}. \tag{1}$$

In the one-constant approximation the nematic free-energy density is given by

$$f_n(\mathbf{r}) = \tfrac{1}{2}K[(\nabla\cdot\mathbf{n})^2 + (\nabla\times\mathbf{n})^2], \tag{2}$$

where K is a nematic elastic constant. The smectic free-energy density is

$$f_s(\mathbf{r}) = c_\parallel|(\mathbf{n}\cdot\nabla - iq_0)\psi|^2 + c_\perp|(\mathbf{n}\times\nabla)\psi|^2 + D|(\mathbf{n}\times\nabla)^2\psi|^2, \tag{3}$$

where $c_\parallel$, $c_\perp$, and D are the smectic elastic constants. The quantity $c_\parallel$ is related to the compressibility smectic elastic constant B: $c_\parallel = Bq_0^{-2}\eta_B^{-2}$, as will be shown later. The corresponding term in $f_s(\mathbf{r})$ is zero if the layer thickness is the

same as in the Sm-*A* phase, i.e., $d_0=2\pi/q_0$. The smectic tilt elastic constant $c_\perp$ measures the cost of tilting the director away from the layer normal. We assume that it is temperature dependent: $c_\perp=c_{\perp 0}(T/T_{AC}-1)$, where T_{AC} is the transition temperature from the Sm-*A* to the Sm-*C* phase in the bulk. In the Sm-*A* phase $c_\perp>0$ and the corresponding term forces the molecules to align perpendicular to the smectic layer. In the Sm-*C* phase $c_\perp<0$ and the corresponding term is minimized if the molecules align parallel to the layers. The final term stabilizes an intermediate tilt of **n** with respect to the normal to the layer in the Sm-*C* phase. In addition, it contains the second derivative of the phase factor $\phi(\mathbf{r})$, a term that resists the bending of the smectic layers. In the bulk Sm-*C* phase the elastic smectic contribution is minimized for the molecular cone angle $\vartheta_B=\arctan\sqrt{|c_\perp|/(2Dq_0^2)}$. We emphasize that the above four elastic constants (one nematic and three smectic) are the minimum set of parameters to describe the major qualitative features of chevron cells.

The surface energy is modeled by the Rapini-Papoular term describing tangential homogeneous anchoring

$$f_a(\mathbf{r})=-\tfrac{1}{2}W_S(\mathbf{n}\cdot\hat{\mathbf{z}})^2. \tag{4}$$

In the limit of strong orientational anchoring ($W_S\to\infty$) the molecules align along the easy axis $\hat{\mathbf{z}}$. Clearly the model can be trivially modified to take into account surface treatments that favor finite pretilt for technological reasons, though we do not address this question in this paper.

Details of the calculation

The calculations are performed in the Cartesian coordinate system. The Sm-*C* liquid crystal is confined between the plates located at $x=-L/2$ and $x=L/2$, as shown in Fig. 1(a). The layers are running in the z direction. The director orientation can be written as

$$\mathbf{n}=(\sin\alpha\ \sin\beta,\sin\alpha\ \cos\beta,\cos\alpha), \tag{5}$$

where α is the angle between the z direction and **n**, and β is the angle between the y direction and the projection of **n** to the xy plane.

We assume that α and β are functions of x only. The smectic density wave enforces the periodicity in the z direction and is expressed as $\psi(\mathbf{r})=\eta_B\exp\{iq_0[z+u(x)]\}$. The displacement vector $u(x)$ describes departures from the planar layer configuration. The periodicity enforced in the z direction is $q_0=2\pi/d_0$ and is established in the Sm-*A* phase.

In the coordinate system chosen for numerical calculations the variables are $\alpha(x)$, $\beta(x)$, and $u(x)$. The chevron structure is usually described in the local coordinate system by the molecular cone angle $\vartheta(x)$, the layer tilt angle $\delta(x)$, and the rotation about the cone $\varphi(x)$ [Fig. 1(b)]. In terms of these angles **n** is expressed as

$$\mathbf{n}=(\cos\delta\ \sin\vartheta\ \sin\varphi-\sin\delta\ \cos\vartheta,\sin\vartheta\ \cos\varphi,\sin\delta\ \sin\vartheta\ \sin\varphi+\cos\vartheta\cos\delta). \tag{6}$$

Comparing expressions (5) and (6) and observing that $du/dx=-\tan\delta$, we find the following relations:

$$\cos\vartheta=\frac{-\tan\delta\ \sin\alpha\ \sin\beta+\cos\alpha}{\sqrt{1+\tan^2\delta}}$$

and

$$\cos\varphi=\frac{\sin\alpha\ \cos\beta}{\sin\vartheta}.$$

There are three important length scales in the problem. These are the following:

(i) $\lambda_\perp=[K/(|c_\perp|q_0^2\eta_B^2)]^{1/2}$ and $\lambda_\parallel=[K/(c_\parallel q_0^2\eta_B^2)]^{1/2}$, measuring the penetration of locally induced nematic bend or twist deformation into the smectic phase in the layer plane ($\lambda_\perp$) and along the layer normal ($\lambda_\parallel$); we regard these as subclasses of the same phenomenon.

(ii) $\lambda_S=K/W_S$, the surface extrapolation length.

(iii) $\lambda_{\rm ch}=2\sqrt{2Dq_0}(c_\parallel|c_\perp|)^{-1/2}$, the chevron tip length scale.

We shall find it convenient to introduce the following dimensionless parameters: (a) the reduced temperature, $t=T/T_{AC}-1$; (b) $|c_\perp|/c_\parallel=a_0|t|=(\lambda_\parallel/\lambda_\perp)^2$; (c) $D_1=D\eta_B^2q_0^4L^2/K$; (d) $D_2=D\eta_B^2q_0^2/K$; (e) $\rho=x/L$; (f) $w=du/dx$. The bulk value of the molecular cone angle and the chevron tip width can be expressed in terms of the dimensionless parameters D_1 and D_2 as $\tan\vartheta_B=L/\lambda_\parallel\sqrt{a_0|t|/(2D_1)}$ and $\lambda_{\rm ch}=2\lambda_\parallel\sqrt{D_2}/\tan\vartheta_B$.

For computational purposes we express the free energy in the dimensionless form. The dimensionless free energy G per unit surface is defined as

$$G=\frac{L}{K}F=\int_{-1/2}^{1/2}[g_n(\rho)+g_s(\rho)]d\rho+g_a(\rho=1/2)+g_a(\rho=-1/2). \tag{7}$$

The quantities in Eq. (7) have the following meanings (the subscript ρ denotes the derivative with respect to ρ):

$$g_n(\rho)=\tfrac{1}{2}(\alpha_\rho^2+\beta_\rho^2\sin^2\alpha) \tag{8}$$

is the dimensionless nematic free-energy density;

$$\begin{aligned}g_s(\rho)=&\frac{L^2}{\lambda_\parallel^2}(w\ \sin\alpha\ \sin\beta+\cos\alpha-1)^2+\frac{L^2}{\lambda_\parallel^2}a_0t[\sin^2\alpha\\&+w^2(\sin^2\alpha\ \cos^2\beta+\cos^2\alpha)-w\ \sin2\alpha\ \sin\beta]\\&+D_1[\sin^2\alpha+w^2(\sin^2\alpha\ \cos^2\beta+\cos^2\alpha)\\&-w\ \sin2\alpha\ \sin\beta]^2\\&+D_2[(\alpha_\rho\cos\alpha\ \sin\beta+\beta_\rho\sin\alpha\ \cos\beta)\\&\times(w\ \sin\alpha\ \sin\beta+\cos\alpha)-(1-\sin^2\alpha\ \sin^2\beta)w_\rho]^2\end{aligned} \tag{9}$$

is the dimensionless smectic free energy; and

$$g_a(\rho)=-\frac{L}{2\lambda_S}\cos^2\alpha \tag{10}$$

is the dimensionless surface orientational anchoring free energy.

The minimization of the free energy G yields three bulk equations:

$$\frac{\partial(g_n+g_s)}{\partial\alpha}-\frac{d}{d\rho}\frac{\partial(g_n+g_s)}{\partial\alpha_\rho}=0, \tag{11}$$

$$\frac{\partial(g_n+g_s)}{\partial\beta}-\frac{d}{d\rho}\frac{\partial(g_n+g_s)}{\partial\beta_\rho}=0, \tag{12}$$

$$\frac{\partial g_s}{\partial w}-\frac{d}{d\rho}\frac{\partial g_s}{\partial w_\rho}=0, \tag{13}$$

and three surface equations for each boundary

$$\left[\pm\frac{\partial(g_n+g_s)}{\partial\alpha_\rho}+\frac{\partial g_a}{\partial\alpha}\right]_{\rho=\pm1/2}=0\,, \tag{14}$$

$$\left[\pm\frac{\partial(g_n+g_s)}{\partial\beta_\rho}+\frac{\partial g_a}{\partial\beta}\right]_{\rho=\pm1/2}=0, \tag{15}$$

$$\left(\frac{\partial g_s}{\partial w_\rho}\right)_{\rho=\pm1/2}=0. \tag{16}$$

The Euler-Lagrange equations are solved numerically using the relaxation method [21]. The layer displacement $u(\rho)$ can be obtained from $w(\rho)$ by integration.

The expression for the free-energy density is expressed more simply in terms of the angles α, β, and w rather than with δ, ϑ, and φ. However, in the limit of small angles it is rather easy to reexpress the free-energy density in terms of the local coordinate system. We now use this set of parameters in order to identify the physical meaning of the dimensionless parameters and length scales that we have introduced. For simplicity we assume no orientational surface anchoring ($\lambda_S\to\infty$). We express the nematic [Eq. (8)] and smectic [Eq. (9)] dimensionless free-energy densities as an expansion in the angles δ, ϑ, and φ for $t<0$. In the spirit of Landau, we include second- and fourth-order terms in these angles. We then obtain for the total free-energy density:

$$\begin{aligned}g=&\tfrac{1}{2}(\delta_\rho^2+\vartheta_\rho^2+\varphi_\rho^2\vartheta^2-2\delta_\rho\vartheta_\rho\varphi-2\varphi_\rho\delta_\rho\vartheta)\\&+\frac{1}{4}\frac{L^2}{\lambda_\parallel^2}(\vartheta^2-\delta^2)^2-\frac{L^2}{\lambda_\perp^2}\vartheta^2\\&+D_1\vartheta^4+D_2(\vartheta_\rho^2\varphi^2+\varphi_\rho^2\vartheta^2).\end{aligned} \tag{17}$$

(We have neglected the fourth-order terms in ϑ and δ in the $\lambda_\perp$ term, because here the quadratic term in ϑ dominates.)

First we consider the case $\vartheta=\vartheta_B=\text{const}$ and write out the Euler-Lagrange equations for δ and φ:

$$\frac{L^2}{\lambda_\parallel^2}\delta(\delta^2-\vartheta_B^2)+\varphi_{\rho\rho}\vartheta_B-\delta_{\rho\rho}=0,$$

$$(1+2D_2)\varphi_{\rho\rho}\vartheta_B-\delta_{\rho\rho}=0.$$

This is the coupled set of equations already discussed by Nakagawa. The solutions for δ and φ are $\delta=\delta_0\tanh(\rho L/\lambda_\delta)$, where $\delta_0=\vartheta_B$ and $\lambda_\delta=2\lambda_\parallel[D_2/\{\vartheta_B^2(1+2D_2)\}]^{1/2}$, and $\varphi=\varphi_0\tanh(\rho L/\lambda_\delta)$, with $\varphi_0=\delta_0/[\vartheta_B(1+2D_2)]$. Since $\delta_0=\vartheta_B$ and D_2 is usually much smaller than 1, the amplitude of φ is not small and the approximation $\varphi\ll1$ is not justified. Nevertheless, from the above result we expect that the typical lengths that describe relaxation of the layer tilt angle and the rotation about the cone are the same. Assuming $D_2\ll1$, we define the characteristic chevron tip length scale as $\lambda_{\rm ch}=2\lambda_\parallel\sqrt{D_2}/\vartheta_B$, which in the limit of small ϑ_B coincides with our original definition.

We also need a length that describes angular relaxation to the cone angle. The Euler-Lagrange equation for ϑ is

$$\begin{aligned}&\frac{L^2}{\lambda_\parallel^2}\vartheta(\vartheta^2-\delta^2)-2\frac{L^2}{\lambda_\perp^2}\vartheta+4D_1\vartheta^3+(1+2D_2)\varphi_\rho^2\vartheta\\&\quad-4D_2\varphi_\rho\vartheta_\rho\varphi-(1+2D_2\varphi^2)\vartheta_{\rho\rho}+\delta_{\rho\rho}\varphi=0\,.\end{aligned} \tag{18}$$

This differential equation cannot be solved analytically. In the bookshelf geometry ($\varphi=\delta=0$), it reduces to

$$\left(\frac{L^2}{\lambda_\parallel^2}+4D_1\right)\vartheta^3-2\frac{L^2}{\lambda_\perp^2}\vartheta-\vartheta_{\rho\rho}=0.$$

Next we assume that $\vartheta=\vartheta_0+\Delta\vartheta(\rho)$ and finally obtain

$$4\frac{L^2}{\lambda_\perp^2}\Delta\vartheta-(\Delta\vartheta)_{\rho\rho}=0\quad\text{and}\quad\vartheta_0^2=\frac{2(L^2/\lambda_\perp^2)}{L^2/\lambda_\parallel^2+4D_1}<\vartheta_B^2.$$

From this, the perturbations in ϑ should die out on the length scale of $\lambda_\perp/2$.

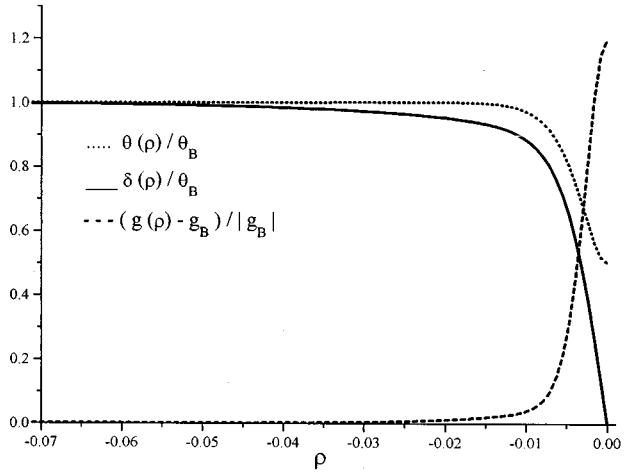

FIG. 2. Numerical results for the spatial variations of the molecular cone angle, the layer tilt angle, and the free-energy density. Dotted line, the molecular cone angle ϑ; full line, the layer tilt angle δ; dashed line, the free-energy density $g(\rho)$; and g_B, the bulk value of the free-energy density. The parameter values are $L^2/\lambda_\parallel^2=10^5$, $a_0=1$, $|t|=0.01$, $D_1=4\times10^4$, $D_2=0.01$, and $L/\lambda_S=0$.

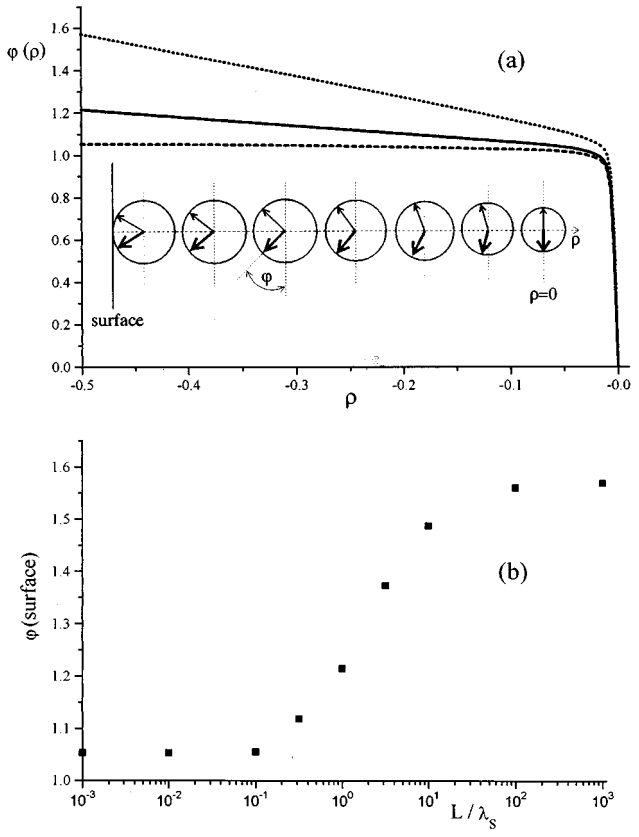

FIG. 3. The rotation of the molecular director about the cone. (a) The director rotation about the cone (φ) for different surface orientational strengths. Dotted line, strong anchoring, $L/\lambda_S=10^3$; full line, medium anchoring, $L/\lambda_S=1$; dashed line, weak anchoring, $L/\lambda_S=10^{-3}$; inset, the **c**-director rotation about the cone at an intermediate value of the surface anchoring strength. Two stable states, both with the same total free energy, are shown. (b) The value of φ at the surface as a function of the surface orientational anchoring strength. In all cases, $L^2/\lambda_\parallel^2=10^5$, $a_0=1$, $|t|=0.01$, $D_1=4\times10^4$, and $D_2=0.01$.

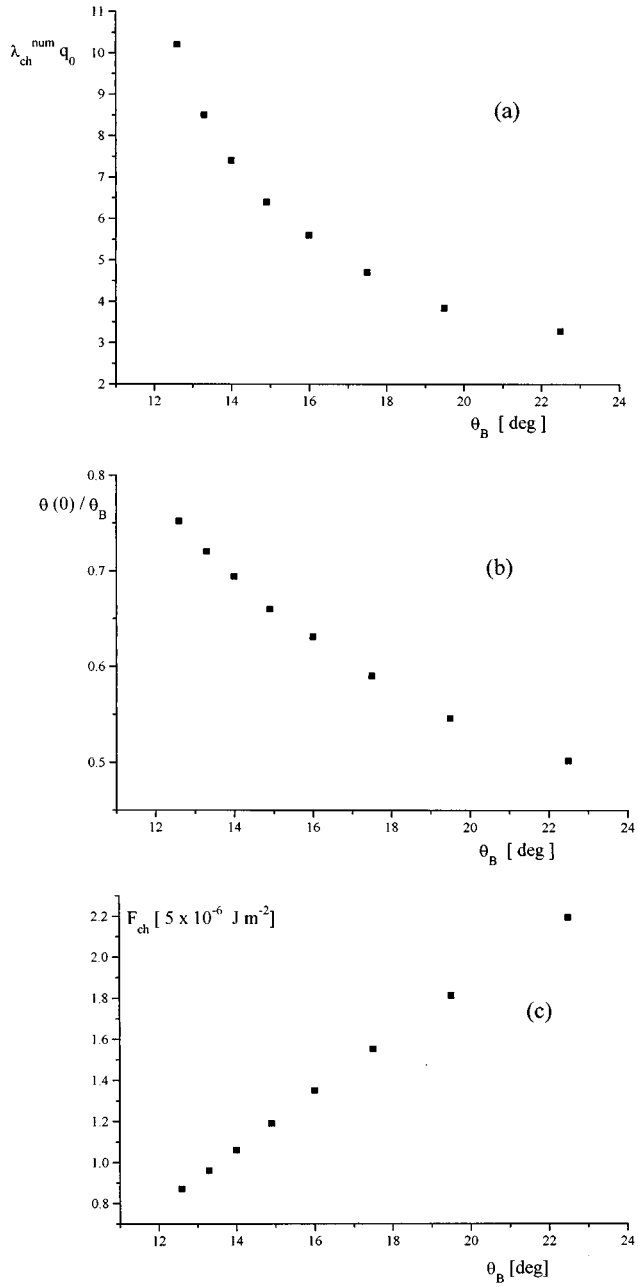

FIG. 4. (a) The width of the chevron tip, (b) the reduction of the molecular cone angle at the chevron tip, and (c) the energy of the chevron interface as a function of ϑ_B at a constant reduced temperature. $L=2$ μm, $K=10^{-11}$ J/m. In all cases: $L^2/\lambda_\parallel^2=10^5$, $a_0=1$, $|t|=0.1$, and $L/\lambda_S=0$.

III. CHEVRON STRUCTURE

A. Parameter values

Typical values for the parameters entering the model are $L\approx2\mu$m and $d_0\sim\lambda_\parallel\approx3$nm [22]. We do not know of any experimental measurements of $a_0|t|$ deep in the Sm-C phase, i.e., far from the Sm-A–Sm-C or N–Sm-C phase transition. As an estimate we use McMillan's [23] estimate that deep in the Sm-A phase $a_0|t|$ is of the order of the ratio between the molecular diameter and the molecular length, and we take $a_0|t|\approx0.1$. The values of $c_\perp$, $c_\parallel$, and D have been measured close to the N–Sm-A–Sm-C multicritical point [24]. From those measurements of $|c_\perp|/c_\parallel$ at different $|t|$ we estimate that $a_0\sim o(1)$. The parameter D_1 is calculated using the values for $a_0|t|$ and $\lambda_\parallel$ and assuming a value for the bulk molecular cone angle. For the materials showing the N–Sm-A–Sm-C phase transition $\vartheta_B\approx20°$. D_2 is obtained from D_1 by noting that $D_2=D_1/(L^2q_0^2)$.

B. Director structure

We have calculated the director structure using the following representative values of the parameters: $L^2/\lambda_\parallel^2=10^5$, $a_0=1$, $|t|=0.01$, $D_1=4\times10^4$, and $D_2=0.01$. Figure 2 shows the numerical results for the spatial variations of the molecular cone angle ϑ and the layer tilt angle δ at a very weak surface orientational anchoring ($L/\lambda_S\to0$). The angles ϑ and δ are equal to the bulk value of the molecular cone angle everywhere except around the chevron tip. This area is enlarged in the figure. Around the chevron tip ϑ is reduced significantly and δ goes to zero.

In Figs. 3(a) and 3(b) the director rotation about the cone is shown. In the middle of the cell $\varphi(0)=0$ or π [Fig. 3(a)].

This is expected, as these two positions are the only ones with $\vartheta(0)\neq 0$ where the director remains continuous over the symmetric cell. Another possibility would be $\vartheta(0)=0$, but the corresponding free energy is greater than in the case of $\varphi(0)=0$ or π with finite $\vartheta(0)$. The director rotates about the cone when moving towards the surface. While the changes in the spatial variation of ϑ and δ caused by the variation of the surface anchoring strength are small, the rotation about the cone strongly depends on the surface orientational anchoring strength as shown in Fig. 3(a). In the case of very strong anchoring the director rotates about the cone by $\pi/2$ so that it is along the z axis at the surface, while with weak anchoring $\varphi\neq\pi/2$ at the surface. The rotation of the projection of the director to the smectic plane (**c** director) is shown in the inset to Fig. 3(a). Thus, although $\delta=\pm\vartheta_B$ everywhere in the cell except around the chevron tip, the director tilts away from the cell plane (x,z). As soon as the director tilts away from the (x,z) plane, there are two distinct stable director states with the same free energy [the inset to Fig. 3(a)]. This bistability is very important and is used in optical applications, where the cell is switched between these states, i.e., between a dark and a bright state.

The value of φ at the surface as a function of the surface orientational anchoring strength is shown in Fig. 3(b). A reasonable value of $W_S=10^{-5}$ J/m^2 [25,26] gives with $K\sim 10^{-11}$ J/m^1 the surface extrapolation length $\lambda_S\approx 1\mu$m, which is just the range of a typical cell thickness used in displays. From Fig. 3(b) we deduce that $\lambda_S\approx 1\mu$m corresponds to an intermediate value of the surface orientational anchoring.

The free-energy density variation $g(\rho)$ is shown in Fig. 2. As expected the free-energy density takes its bulk value everywhere except close to the chevron tip. In that region it increases significantly. Assuming $L=2$ μm and $K=10^{-11}$ J/m^1, the excess energy associated with the chevron interface is 3.5×10^{-7} J/m^2. The free-energy density even becomes positive around the chevron tip, which suggests that local smectic elastic distortions might be strong enough to cause a substantial decrease in the smectic order parameter η.

We also examine the length scale defining the chevron tip, the excess energy of the chevron interface, and the reduction of the molecular cone angle at the chevron tip as a function of the elastic constant D at $|t|=0.1$, i.e., well inside the Sm-C phase. The parameters $c_\perp(T)$ and D determine the bulk value of the molecular cone angle and the characteristic chevron interface width. We therefore plot the numerical results as a function of ϑ_B at constant reduced temperature. The chevron tip length scale [Fig. 4(a)] is obtained by comparison with the hypothetical form $\delta=\delta_s\tanh(\rho L/\lambda_{ch})$, where δ_s is the value of δ at the cell surface. In practice we use as a criterion for chevron width that distance over which δ rises from 0 to $\delta_s\tanh 1$. The ratio between the numerically calculated chevron tip length scale and λ_{ch} is essentially constant for all ϑ_B and equal to 1.10 ± 0.05. The approximation $\delta=\delta_s\tanh(\rho L/\lambda_{ch})$ is thus quite good. From Fig. 4(a) we also see that far from the Sm-A–Sm-C transition temperature the chevron tip length scale is of the order of the layer thickness and of the order 10^{-3} of the cell thickness. Our continuum model should be valid even for such small λ_{ch}, as the short axes of the molecules are considerably smaller than the layer thickness and so the number of molecules in the deformedregion of each layer is still reasonably large. The energy of the chevron interface is plotted in Fig. 4(c) as a function of ϑ_B. The energy increases for narrower chevron tips and shows linear dependence on ϑ_B at a constant reduced temperature. This dependence can also be obtained from Eq. (17), where the leading term in the chevron energy is $F_{ch}=KG_{ch}/L\propto c_\perp\lambda_{ch}\vartheta_B^2\propto\vartheta_B$.

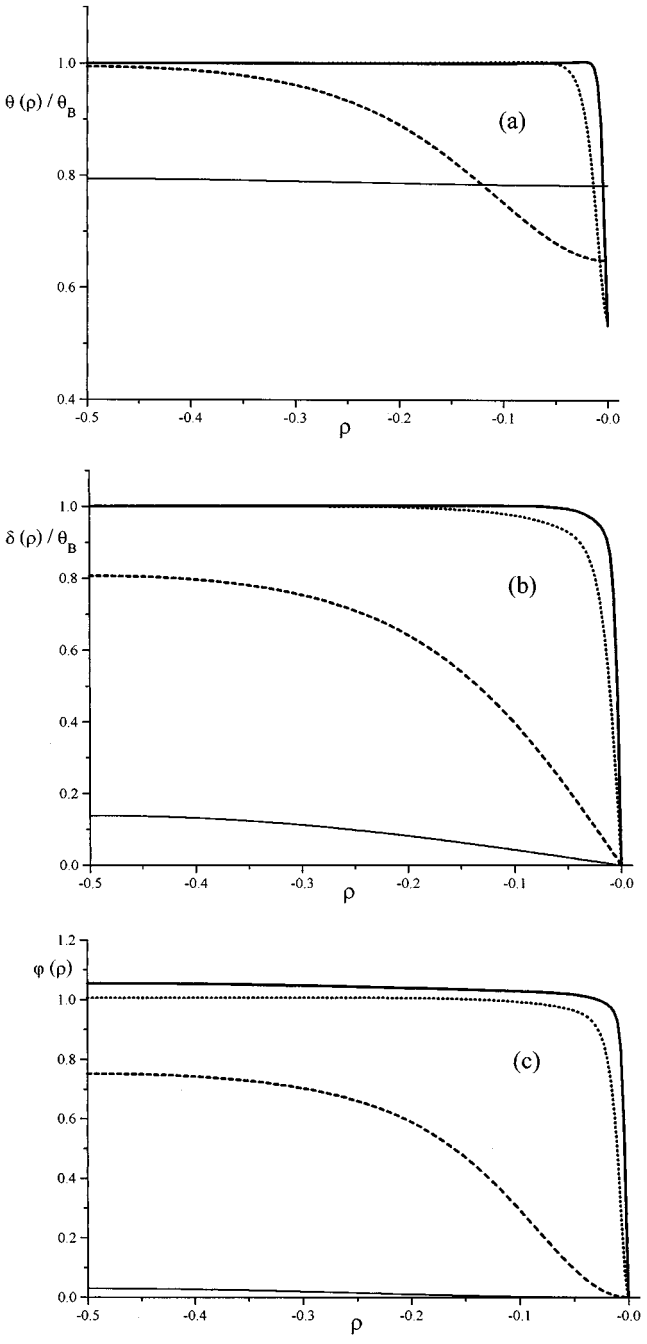

FIG. 5. Temperature dependence of the chevron structure. Thick full line, $|t|=0.01$; dotted line, $|t|=0.001$; dashed line, $|t|=10^{-5}$; and thin full line, $|t|=2.6\times 10^{-6}$. Spatial variations of the (a) molecular cone angle, (b) layer tilt angle, and (c) rotation about the cone. In all cases, $L^2/\lambda_\parallel^2=10^5$, $a_0=1$, $D_1=4\times 10^4$, $D_2=0.01$, and $L/\lambda_S=0$.

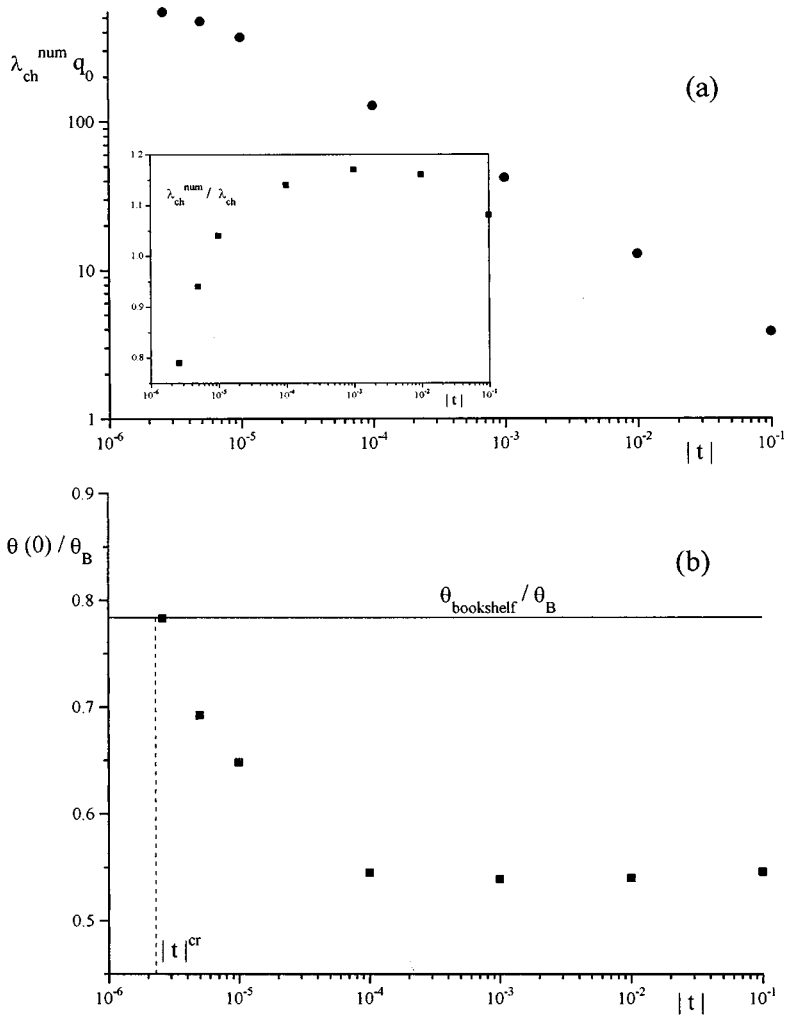

FIG. 6. (a) Temperature dependence of the chevron tip width. Inset, temperature dependence of the ratio between the numerically calculated chevron tip width (λ_{ch}^{num}) and the characteristic length λ_{ch}. (b) Temperature dependence of the reduction of the molecular cone angle at the chevron tip. Line, the molecular tilt in the bookshelf geometry above the threshold temperature for the chevron formation and below the Sm-A–Sm-C transition temperature. In all cases, $L^2/\lambda_{\parallel}^2=10^5$, $|t|^{cr}=2.5\times10^{-6}$, $D_1=4\times10^4$, $D_2=0.01$, and $L/\lambda_S=0$.

C. Temperature dependence

The results for temperature dependence of δ, ϑ, and φ for a chosen value of D, corresponding to $\vartheta_B=19.5°$ at $|t|=0.1$ in Fig. 4(a), are shown in Figs. 5(a)–5(c). The plots show that the chevron tip width is increased when temperature approaches the Sm-A–Sm-C transition temperature.

The temperature dependence of the chevron tip width and the ratio between the numerically calculated chevron tip width (λ_{ch}^{num}) and the characteristic length λ_{ch} are shown in Fig. 6(a). We observe that close to the phase transition temperature the chevron tip width is smaller than λ_{ch}. In the following we show that close to the phase transition the approximation $\delta=\delta_s\sin(\pi\rho)$ is better than $\delta=\delta_s\tanh(\rho L/\lambda_{ch})$. The temperature dependence of the decrease in the molecular cone angle at the chevron tip is shown in Fig. 6(b). In Fig. 7 the energy of the chevron interface is plotted. It shows a power-law dependence on the reduced temperature with an exponent of 3/2 that can be obtained from Eq. (17), where the leading term in the energy of the chevron is $F_{ch}=KG_{ch}/L\propto c_{\perp}\vartheta_B^2\lambda_{ch}+c_{\parallel}\vartheta_B^4\lambda_{ch}\propto|t|^{3/2}$, since $c_{\perp}\propto|t|$, $\vartheta_B\propto|t|^{1/2}$, and $\lambda_{ch}\propto\vartheta_B^{-1}\propto|t|^{-1/2}$. The plot of numerically computed values in Fig. 7 gives an exponent of 1.52 ± 0.02, which gives a check on the consistency of calculation.

To estimate the threshold temperature for the chevron formation we have used the following procedure. Close to the Sm-A–Sm-C phase transition the angles α and β and the variable w are small. The symmetric chevron structure requires $\beta(0)=0$ and $w(0)=0$. We consider only free surfaces at $\rho=\pm1/2$ (no orientational, only positional anchoring: $L/\lambda_S=0$), which leads to $\alpha_\rho(\pm1/2)=\beta_\rho(\pm1/2)=w_\rho(\pm1/2)=0$. In addition, the variable α is symmetric around the chevron interface, while w and β are antisymmetric. Then the variables can be written as

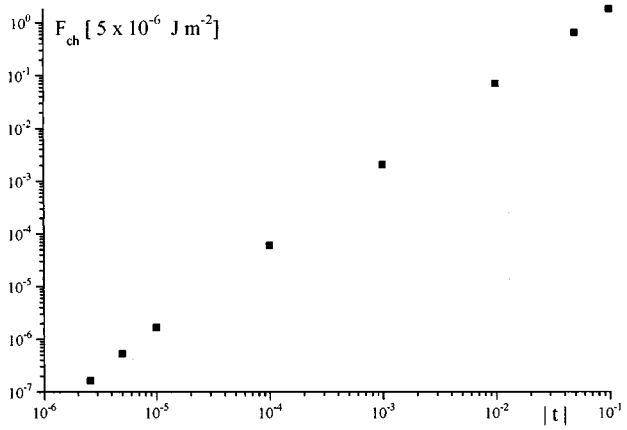

FIG. 7. Temperature dependence of the excess free energy associated with the chevron interface. $D_1=4\times10^4$, $D_2=0.01$, $L=2$ μm, $K=10^{-11}$ J/m, $L^2/\lambda_{\parallel}^2=10^5$, and $L/\lambda_S=0$.

$$\alpha(\rho)=\sum_{k=0}^{\infty}\alpha_k\cos 2k\pi\rho\approx\alpha_0, \tag{19}$$

$$\beta(\rho)=\sum_{k=0}^{\infty}\beta_k\sin k\pi\rho\approx\beta_1\sin\pi\rho, \tag{20}$$

$$w(\rho)=\sum_{k=0}^{\infty}w_k\sin k\pi\rho\approx w_1\sin\pi\rho. \tag{21}$$

We now use the fact that the leading term dominates close to the phase transition.

To obtain the amplitudes α_0, β_1, and w_1 the free-energy density [Eq. (7)] has to be expanded up to the fourth order in α, β, and w. After integration we obtain the following expression for the total free energy of the cell:

$$\begin{aligned}G=&\left(\frac{L^2}{\lambda_\parallel^2}a_0t\right)\alpha_0^2+\frac{1}{2}\left(\pi^2D_2+\frac{L^2}{\lambda_\parallel^2}a_0t\right)w_1^2\\&+\frac{1}{4}\left(\frac{L^2}{\lambda_\parallel^2}+4D_1\right)\alpha_0^4+\tfrac{3}{8}D_1w_1^4+D_1\alpha_0^2w_1^2\\&-\left(\frac{L^2}{\lambda_\parallel^2}a_0t+\pi^2D_2\right)\alpha_0w_1\beta_1+\frac{\pi^2}{2}(1/2+D_2)\alpha_0^2\beta_1^2.\end{aligned}$$

This expression is minimized for the following nonzero values of the amplitudes α_0, w_1, and β_1:

$$w_1^2=\frac{-\frac{L^4}{\lambda_\parallel^4}a_0t+\left\{-\pi^2D_2+\left(\frac{L^2}{\lambda_\parallel^2}a_0t+\pi^2D_2\right)^2\frac{1}{\pi^2(1/2+D_2)}\right\}\left(\frac{L^2}{\lambda_\parallel^2}+4D_1\right)}{2D_1^2+\frac{3}{2}D_1\frac{L^2}{\lambda_\parallel^2}}, \tag{22}$$

$$\alpha_0^2=\frac{-2\left(\frac{L^2}{\lambda_\parallel^2}a_0t+D_1w_1^2\right)}{\frac{L^2}{\lambda_\parallel^2}+4D_1}, \tag{23}$$

$$\beta_1=\frac{\pi^2D_2+\frac{L^2}{\lambda_\parallel^2}a_0t}{(1/2+D_2)\pi^2}\frac{w_1}{\alpha_0}. \tag{24}$$

A real value for w_1 is obtained only for $t<t^{\rm cr}$, where $t^{\rm cr}$ is obtained from Eq. (22):

$$-\frac{L^4}{\lambda_\parallel^4}a_0t^{\rm cr}+\left\{-\pi^2D_2+\left(\frac{L^2}{\lambda_\parallel^2}a_0t^{\rm cr}+\pi^2D_2\right)^2\frac{1}{\pi^2(1/2+D_2)}\right\}\times\left(\frac{L^2}{\lambda_\parallel^2}+4D_1\right)=0\,.$$

For $L^2/\lambda_\parallel^2=10^5$, $a_0=1$, $D_1=4\times10^4$, and $D_2=0.01$ this value is $t^{\rm cr}=-2.5\times10^{-6}$. The critical temperature for the chevron formation increases for materials with a smaller compressibility constant or a smaller value of the bulk molecular cone angle deep in the Sm-C phase. The transition temperature to the Sm-C phase is not shifted from its bulk value. As soon as $t<0$, the bookshelf geometry, where the molecules are tilted by $\alpha_0=\vartheta_B/[1+(L^2/\lambda_\parallel^2)/(4D_1)]^{1/2}$ in the (x,y) plane, becomes stable. The transition is second order. The chevron structure can exist below $t^{\rm cr}$. The bookshelf structure with tilted molecules remains metastable, while the chevron structure is the structure with the minimum total free energy. We have checked that the numerical results confirm the analytical predictions.

D. Comparison with other models of chevron behavior

First we shall compare our model with the Limat free-energy density. For that purpose we rewrite the dimensionless free energy [Eq. (17)] in the dimensional form and assume that $\vartheta=\vartheta_0=$const. For the nematic free-energy density we obtain

$$f_n=\tfrac{1}{2}K[\,\delta_x^2+\vartheta_0^2\varphi_x^2-2\,\vartheta_0\delta_x\varphi_x\cos\varphi]; \tag{25}$$

and for the smectic free-energy density,

$$\begin{aligned}f_s=&q_0^2\eta_B^2c_\parallel\left(\frac{\vartheta_0^2}{2}-\frac{\delta^2}{2}\right)^2-|c_\perp|q_0^2\eta_B^2\vartheta_0^2+Dq_0^4\eta_B^2\vartheta_0^4\\&+Dq_0^2\eta_B^2\varphi_x^2\vartheta_0^2\cos^2\varphi.\end{aligned} \tag{26}$$

Considering only the nonconstant contributions, the total free-energy density is

$$\begin{aligned}f=&\tfrac{1}{2}K[\,\delta_x^2+(1+D_2\cos^2\varphi)\,\vartheta_0^2\varphi_x^2-2\,\vartheta_0\delta_x\varphi_x\cos\varphi]\\&+q_0^2c_\parallel\eta_B^2\left(\frac{\vartheta_0^2}{2}-\frac{\delta^2}{2}\right)^2.\end{aligned} \tag{27}$$

This expression can now be compared with the Limat free-energy density:

$$f_{\mathrm{LIM}}=\tfrac{1}{2}K(\delta_x^2+n\vartheta_0^2\varphi_x^2-2m\vartheta_0\delta_x\varphi_x\cos\varphi)+B\left(\frac{\delta_0^2}{2}-\frac{\delta^2}{2}\right)^2 + (\text{chiral term}), \tag{28}$$

where n and m measure the departures from the uniaxial approximation. Comparing the free-energy density expressions (27) and (28) we find the following relations:

$$n=1+D_2\cos^2\varphi,\quad m=1,\quad B=c_{\parallel}q_0^2\eta_B^2.$$

The model of Clark and co-workers [1,4] can be obtained from the Limat model in the limit $n=m=1$, that is, for $D_2=0$. This, however, is an unphysical value. In realistic cases D_2 is small (about 0.01) and far from the Sm-A–Sm-C phase transition the chevron tip width is small compared to the cell thickness ($\lambda_{\mathrm{ch}}^{\mathrm{num}}\approx 10^{-3}L$). In that region the assumptions of Clark and co-workers are justified. But this model essentially loses the information on the energy of the chevron interface. It also predicts that there is no director rotation on the cone away from the cell plane [the (x,z) plane in our coordinate system] if the layer tilt angle equals the molecular cone angle. In their model the pretilt of the director results from the fact that the layer tilt angle is smaller than the molecular cone angle. We have shown that the continuity of the molecular director over a chevron tip with finite thickness is a sufficient condition for the director pretilt and that the degree of pretilt strongly depends on the surface treatment [Figs. 3(a) and 3(b)].

Nakagawa's solution can also be obtained from the Limat model in the limit of small φ. Limat has shown that the Nakagawa model can be applied only in the limit of $\delta_0/\vartheta_0\ll 1$, where δ_0 is the layer tilt angle far from the chevron tip. We have shown that far from the Sm-A–Sm-C phase transition and at zero orientational surface anchoring the spatial dependences of δ and φ are described well by $\delta=\delta_0\tanh(\rho L/\lambda_{\mathrm{ch}})$ and $\varphi=\varphi_0\tanh(\rho L/\lambda_{\mathrm{ch}})$. But the amplitudes δ_0 and φ_0 need not be small and the condition $\delta_0\ll\vartheta_0$ is not necessary to obtain a finite pretilt of the molecular director. Our results also show that far from the phase transition the chevron tip width is of the order of layer thickness. It can be argued, therefore, that the reduction of the molecular cone angle at the chevron tip can be neglected, since it happens on such a small length scale. We have checked that the approximation with constant ϑ does not affect the amplitudes of δ and φ significantly. It does affect, though, the free energy of the chevron interface, which is about twice as great if we assume ϑ to be constant.

De Meyere and co-workers [11,12] have considered spatial variations of the molecular cone angle. They have assumed the following relation between δ and ϑ: $\cos\vartheta=\nu\cos\delta$, where $\nu=l_0/l_m$, l_0 is the layer thickness along the z direction, and l_m is the molecular length that changes with temperature. At the chevron tip $\delta=0$; therefore $\cos\vartheta=\nu$. If $\nu=1$, as in our model, ϑ should be zero at the chevron tip. But we treat ϑ and δ as independent variables. In the expression for the free-energy density there are two competing terms that determine the cone angle value: the compression energy and the $c_{\perp}$ term. In the small-angle approximation the first one is proportional to $c_{\parallel}(\delta^2-\vartheta^2)^2$ and the second to $-|c_{\perp}|\vartheta^2$ [see Eq. (26)]. So, although the $c_{\perp}$ elastic constant is about ten times smaller than $c_{\parallel}$ (far from the Sm-A–Sm-C phase transition), the second term is more important. This explains why the molecular cone angle decreases at the chevron tip; it does not, however, go completely to zero.

IV. CONCLUSIONS

We have used Landau–de Gennes theory to describe the chevron structure in uniform and symmetric achiral Sm-C cells. The model is conceptually extremely simple. We find that the chevron is a thermodynamical equilibrium structure. The model has permitted calculation of the essential properties of the chevron. Among such properties are the existence of bistability of the optical axis, the energy and thickness of the chevron interface, and the threshold condition for chevron formation. In our calculations the effect of layer mismatch between the bulk and the surface has been ignored, and for this reason the layer tilt δ and the cone angle ϑ_B are very closely equal. Relaxing this condition alters this conclusion.

There are a number of other related models that treat chevron properties in Sm-C liquid-crystal cells. Many of these models require simplifying assumptions in order to derive a tractable set of equations. These simplifying assumptions are not required in the model we have used. We have elaborated the connection between the Landau–de Gennes theory and other models that may be regarded as special cases within this more general paradigm.

We have also studied the influence of surface orientational anchoring on the pretilt of the molecular director. By contrast with the work of other authors [1,9–11] we have shown that pretilt is obtained even when the molecular cone angle equals the layer tilt angle. In this special case the pretilt is a consequence of the fact that at the chevron tip a finite angle between the layer normal and the director is favored. This tilt propagates to the cell boundary. Finally we note that in practice the chevron tip is very sharp—its width is approximately $10^{-3}L$, far from the Sm-A–Sm-C phase transition—and there is a significant increase in the free-energy density around the tip. It seems possible, therefore, that the local smectic elastic distortions might be strong enough to cause a substantial variation of the smectic order parameter. We plan to investigate this and other chevron properties in future work.

[1] T.P. Rieker, N.A. Clark, G.S. Smith, D.S. Parmer, E.B. Sirota, and C.R. Safinya, Phys. Rev. Lett. **59**, 2658 (1987).
[2] Y. Ouchi, J. Lee, H. Takezoe, A. Fukuda, K. Kondo, T. Kitamura, and A. Mukoh, Jpn. J. Appl. Phys. **27**, L725 (1988).
[3] M. Cagnon and G. Durand, Phys. Rev. Lett. **70**, 2742 (1993).
[4] N.A. Clark and T.P. Rieker, Phys. Rev. A **37**, 1053 (1988).
[5] N.A. Clark, T.P. Rieker, and J.E. Maclennan, Ferroelectrics **85**, 79 (1988).
[6] J. E. Maclennan, M. A. Handshy, and N. A. Clark, Liq. Cryst. **7**, 787 (1990).
[7] P.C. Willis, N.A. Clark, and C.R. Safinya, Liq. Cryst. **11**, 581 (1992).

[8] M. Nakagawa and T. Akahane, J. Phys. Soc. Jpn. **55**, 1516 (1986).
[9] M. Nakagawa, Displays **11**, 67 (1990).
[10] J. Sabater, J.M.S. Pena, and J.M. Otón, J. Appl. Phys. **77**, 3023 (1995).
[11] A. De Meyere, H. Pauwels, and E. De Ley, Liq. Cryst. **14**, 1269 (1993).
[12] A. De Meyere and I. Dahl, Liq. Cryst. **17**, 379 (1994).
[13] I. Dahl and S.T. Lagerwall, Ferroelectrics **58**, 215 (1984).
[14] I. Dahl, Ferroelectrics **113**, 121 (1991).
[15] L. Limat, J. Phys. France II **5**, 803 (1995).
[16] P.G. de Gennes, Solid State Commun. **10**, 753 (1972).
[17] J. Chen and T.C. Lubensky, Phys. Rev. A **14**, 1202 (1976).
[18] F. M. Leslie, I. W. Stewart, and M. Nakagawa, Mol. Cryst. Liq. Cryst. **198**, 443 (1991).
[19] T. Carlsson, I. W. Stewart, and F. M. Leslie, J. Phys. A **25**, 2371 (1992).
[20] S. Kralj and T.J. Sluckin, Phys. Rev. E **48**, 3244 (1994).
[21] W.H. Press, B.P. Flannery, S.A. Teukolsky, and W.T. Vetterling, *Numerical Recipes* (Cambridge University Press, Cambridge, England, 1986).
[22] P.G. de Gennes, *The Physics of Liquid Crystals* (Clarendon, Oxford, England, 1974).
[23] W.L. McMillan, Phys. Rev. A **7**, 1673 (1973).
[24] L.J. Martinez-Miranda, A.R. Kortan, and R.J. Birgeneau, Phys. Rev. Lett. **56**, 2264 (1986).
[25] A. Rastegar, I. Muševič, and M. Čopič, Ferroelectrics **181**, 1157 (1996).
[26] G. Durand, Liq. Cryst. **14**, 159 (1993).